AJNR Am J Neuroradiol 21:810–816, May 2000

Spatial Relationship between Vestibular Schwannoma and Facial Nerve on Three-dimensional T2-weighted Fast Spin-echo MR Images

Sabine Sartoretti-Schefer, Spyros Kollias, and Anton Valavanis

BACKGROUND AND PURPOSE: **During surgical removal of a vestibular schwannoma, correct identification of the facial nerve is necessary for its preservation and continuing function. We prospectively analyzed the spatial relationship between vestibular schwannomas and the facial nerve using 3D T2-weighted and postcontrast T1-weighted spin-echo (SE) MR imaging.**

METHODS: **Twenty-two patients with a unilateral vestibular schwannoma were examined with MR imaging. The position and spatial relationship of the facial nerve to adjacent tumor within the internal auditory canal (IAC) and cerebellopontine angle cistern (CPA) were assessed on multiplanar reformatted 3D T2-weighted fast spin-echo (FSE) images and on postcontrast transverse and coronal T1-weighted SE images. The entrance of the nerve into the bony canal at the meatal foramen and the nerve root exit zone along the brain stem were used as landmarks to follow the nerve course proximally and distally on all images.**

RESULTS: **The spatial relationship between vestibular schwannoma and facial nerve could not be detected on postcontrast T1-weighted SE images. In 86% of the patients, the position of the nerve in relation to the tumor was discernible on multiplanar reformatted 3D T2-weighted FSE images. In tumors with a maximal diameter up to 10 mm, the entire nerve course was visible; in tumors with a diameter of 11 to 24 mm, only segments of the facial nerve were visible; and in tumors larger than 25 mm, the facial nerve could not be seen, owing to focal nerve thinning and obliteration of landmarks within the IAC and CPA.**

CONCLUSION: **Identification of the facial nerve and its position relative to an adjacent vestibular schwannoma is possible on multiplanar reformatted 3D T2-weighted FSE images but not on postcontrast T1-weighted SE images. Detection of this spatial relationship depends on the tumor's size and location.**

During surgical removal of a vestibular schwannoma, correct identification of the course of the facial nerve adjacent to the tumor is crucial in order to preserve the nerve and its function (1, 2). According to common microsurgical anatomic descriptions, it is a widely accepted operative strategy to identify three segments of the facial nerve: a medial segment from the nerve root exit zone to the medial tumor border, a lateral segment from the lateral tumor border to the entrance of the nerve into the bony canal, and a third segment directly adjacent to the tumor (intervening segment) (1–5). Depending on the operative route (transotic, suboccipital, or middle cranial fossa approach), the facial nerve is first identified lateral to the tumor along the lateral segment within the distal internal auditory canal (IAC) or medial to the tumor along the medial segment (1–3) and subsequently along the intervening segment. Many investigators believe that if the facial nerve is identified both medially and laterally to the tumor (ie, along its medial and lateral segments), the chance of preserving the intervening facial nerve segment increases (2, 3). Identification of the intervening segment may, however, precede identification of the medial segment, especially in the transotic approach (1).

Identification of the seventh nerve lateral to the tumor is often preferred, because the facial nerve invariably enters the facial canal at the anterosuperior quadrant of the lateral margin of the meatus and therefore is usually easiest to locate in this region (1, 2). At a more medial location, the degree of nerve displacement is more variable, depending primarily on the site of origin and the growth characteristics of the tumor (6, 7).

The nerve is splayed around the anterior tumor capsule and therefore is often flattened as thin as a membrane along the intervening segment (1, 2).

Received June 18, 1999; accepted after revision November 15.

From the Institute of Neuroradiology, University Hospital of Zürich, Frauenklinikstrasse 10, CH-8091 Zürich, Switzerland.

Address reprint requests to Sabine Sartoretti-Schefer, MD.

For this reason, identifying the nerve is very difficult along the intervening segment. Additionally, dense adhesions between the tumor capsule, arachnoid, dura, and facial nerve are common along the intervening segment (1, 2, 5–7) and make identification of the intervening facial nerve segment even more difficult (2). Histologic studies of nerves that have ruptured during separation from a tumor have shown tumor cells between facial nerve fibers (1), especially in tumors with diameters greater than 1.5 cm. Tumors less than 1.5 cm in diameter rarely infiltrate the facial nerve (1).

In healthy volunteers, the facial nerve as well as the cochlear, inferior, and superior vestibular nerve have a constant position within the lateral IAC. Relative to the IAC, the facial nerve is located anterosuperiorly, the cochlear nerve anteroinferiorly, the superior vestibular nerve posterosuperiorly, and the inferior vestibular nerve posteroinferiorly. Laterally, these nerve segments are separated by transverse and vertical bony ridges (3, 4, 6–8).

Vestibular schwannomas most frequently arise in the posteriorly placed vestibular nerves. Intraoperative neurosurgical observations confirm that these tumors usually displace the facial nerve anteriorly (in about 98% of cases) (1, 2). Variability in the direction of tumor growth arising from the vestibular nerves may result in direct anterior, anterosuperior, or anteroinferior displacement of the facial nerve (1–3, 7). In 2% of cases, the facial nerve is found along the posterior surface of the tumor (2). Rare tumors arising from the cochlear nerve could displace the facial nerve superiorly and posteriorly, whereas tumors growing superiorly from the superior vestibular nerve could displace the facial nerve inferiorly (2, 7).

In this prospective study, our goal was to analyze the spatial relationship between vestibular schwannomas and the adjoining facial nerve on very thin reformatted 3D T2-weighted fast spin-echo (FSE) MR images and on contrast-enhanced transverse and coronal T1-weighted SE images. We compared multiplanar reconstructions of very thin 3D T2-weighted images with postcontrast thin and overlapped T1-weighted SE images for their ability to depict the course of the facial nerve at the lateral and medial tumor border and along the tumor surface (ie, along the medial, lateral, and intervening nerve segments). We also tried to determine which additional tumor characteristics influence the likelihood of being able to identify the facial nerve (ie, size, position within the cerebellopontine angle [CPA] cistern or IAC, and thinning and flattening of the facial nerve).

Methods

Twenty-two patients (nine men and 13 women; mean age, 55 years; range, 39–76 years) with unilateral vestibular schwannomas were examined on a 1.5-T MR unit. The diagnosis of vestibular schwannoma was established on the basis of clinical presentation (sudden acute unilateral hearing loss and/or chronic progressive hearing loss) and on typical presentation of the tumor on follow-up (9 to 45 months) postcontrast T1-weighted SE MR studies, obtained in 15 patients (strongly and usually homogeneously enhancing tumor arising from the vestibulocochlear nerve, widened IAC and expansion within the CPA cistern, and cystic degeneration (in large tumors) (9–11). The vestibular schwannomas had an entirely intrameatal location in five patients and an intra- and extrameatal location in 17 patients. The mean maximal tumor diameter was 15 mm (range, 3–30 mm). A phased-array dual surface coil with a diameter of 5 in was applied to both ears.

A coronal 3D FSE T2-weighted series (4000/150/1 [TR/TE/excitations[) was acquired with the following parameters: 40 to 70 sections; section thickness, 0.7 mm; echo train length, 48; three slab overlap sections; matrix, 512 × 256; acquisition time, 8:30 minutes. Secondary multiplanar reformations parallel and perpendicular to the course of the facial nerve within the CPA cistern and the IAC were done with a voxel size of 0.4 × 0.4 × 0.6 mm on a Sun workstation (Sun Computer, Mountain View, CA). Transverse and coronal postcontrast T1-weighted SE images (500–600/15–16/4) were obtained with a section thickness of 3 mm in an overlapped fashion with a gap of −1 mm.

For both postcontrast T1-weighted SE sequences and contiguously reformatted oblique transverse, sagittal, and coronal 3D T2-weighted FSE sequences, the course of the facial nerve was assessed on multiple images at three segments: along the medial segment (from the exit of the nerve from the brain stem to the medial tumor border), along the lateral segment (from the lateral tumor border to the entrance of the nerve into the bony facial nerve canal), and, finally, along the intervening segment (where tumor and nerve were in direct contact). Additionally, the direction of nerve displacement and the diameter of the nerve in relation to the diameter of the contralateral facial nerve were analyzed. A nerve was considered to be focally thinned if its diameter was less than that of the contralateral normal facial nerve. The signal intensity of both ipsilateral and contralateral facial nerves was assessed visually and compared, as precise measurements of the signal intensity were not reliable owing to partial volume effects.

Image analysis was performed by two experienced neuroradiologists who were asked to determine the position and course of the entire facial nerve along the different segments on all images available. All contiguously reformatted images were analyzed to identify the facial nerve correctly. Consensus was obtained in all cases.

Results

The results of our study are presented in (Tables 1 through 3). On postcontrast T1-weighted SE images, neither the spatial relationship between nerve and tumor nor focal nerve thinning could be identified (Figs 1A and 2A). On multiplanar 3D T2-weighted reformatted FSE images, identification of the facial nerve adjacent to the tumor was possible (Figs 1B–F, 2B–E, 3, and 4).

In three patients with intra- and extrameatal tumor with maximal diameters of 25 mm, 26 mm, and 30 mm, respectively, the facial nerve could not be distinguished, as the tumor filled the entire IAC as well as the CPA cistern. In two patients with maximal tumor diameters of 3 mm and 11 mm, respectively, the entire facial nerve could be seen (Figs 1B–F and 3A–D).

In patients with large tumors (mean maximal diameter, 24 mm) within the CPA cistern, only identification of the lateral nerve segment was possible. Among these tumors, identification of the medial

Table 1: Identification of different facial nerve segments (medial, lateral, and intervening) adjacent to a vestibular schwannoma

Identification of Facial Nerve along Different Segments	No. (%) Patients	Mean Maximal Tumor Diameter (mm)	Maximal Tumor Diameter of the Different Tumors (mm)
Facial nerve not identified	3 (14)	27	25, 26, 30
Only medical facial nerve segment identified (intervening and lateral segments not depicted)	3 (14)	12.3	10, 12, 15
Only lateral facial nerve segment identified (both tumors located within the CPA cistern, intervening and medical segments not depicted)	2 (9)	24	18, 30
Medial and lateral facial nerve segment identified (intervening segment not depicted)	12 (55)	12.8	11, 12, 12, 12, 12, 12, 13, 13, 13, 14
Medial, lateral, and intervening facial nerve segments identified	2 (9)	7	3, 11

Note.—CPA indicates cerebellopontine angle.

Table 2: Location of different facial nerve segments

Position of Facial Nerve	No. (%) Patients
At the medial tumor border	17 (77)
At the lateral tumor border to the distal intrameatal nerve segment	16 (73)
Along the intervening segment	2 (9)

Table 3: Spatial relationship between facial nerve and adjacent vestibular schwannoma

Position of Facial Nerve in Relation to Adjacent Vestibular Schwannoma	No. (%) Patients
Anterosuperior	17 (77)
Anteroinferior	1 (4.5)
Posterosuperior	1 (4.5)
Nonvisualization of facial nerve	3 (14)

segment was not achieved. If the tumor originated within the IAC, even small tumors filled and obstructed the entire IAC, prohibiting identification of the lateral and intervening nerve segments.

Focal thinning of the facial nerve segment lateral to the tumor and/or of the intervening segment was identified in nine (41%) of patients (Figs 1B–F and 2B–E). These thinned nerve segments had slightly increased signal intensity on 3D T2-weighted FSE images relative to the normal-sized contralateral nerve segments. Identification of the different nerve segments was most easily achieved on parasagittal images perpendicular to the course of the facial nerve within the IAC and the CPA cistern, since, on these images, it was possible to simultaneously distinguish multiple or all four nerves (namely, the facial nerve, the inferior and superior vestibular nerves, and the cochlear nerve) within the IAC. However, in six (27%) of the patients, oblique coronal and transverse images parallel to the nerve course were necessary in order to correctly assess the position of the nerve adjacent to the vestibular schwannoma. Additionally, in 16 patients, oblique transverse and coronal images were analyzed to confirm the position of the nerve as seen on the oblique sagittal images (Figs 1–4).

Discussion

To date, the spatial relationship between a vestibular schwannoma and an adjacent facial nerve cannot be distinguished on postcontrast T1-weighted SE images, even if very thin and overlapping sections are acquired. Even parasagittally acquired images are not helpful (8–12). Preservation of the facial nerve function during surgical removal of a tumor requires correct identification of the nerve medial and lateral to the tumor as well as along the intervening segment (1, 2). Preoperative delineation of the nerve and its position in relation to the tumor on appropriate MR images could help the neurosurgeon more easily identify the nerve intraoperatively. The nerve is usually shifted by the tumor in predictable directions and often is focally thinned and splayed as well (1–3, 5–7). Most commonly, a vestibular schwannoma shifts the facial nerve to an anterosuperior position as compared with its normal position, as seen in healthy volunteers (1, 2). Similarly, the facial nerve may be displaced in an anteroinferior or anterior position, or, rarely, in a posterior position, depending on the growth characteristics of the vestibular schwannoma and which division of the vestibulocochlear nerve is involved (1–7). In 17 (77%) of our patients, the nerve was shifted to an anterosuperior position. However, in one patient (4.5%) the nerve was located anteroinferiorly, and in another patient (4.5%) it was shifted posterosuperiorly. In this latter patient, the tumor probably originated from the cochlear nerve. The facial nerve was not visible in three (14%) of our patients.

Our aim in this prospective study was to determine which factors influence the spatial relationship between facial nerve and tumor on MR images. Is the optimal delineation of this spatial relationship dependent on technical parameters (ie, on differences in the MR sequence performed or

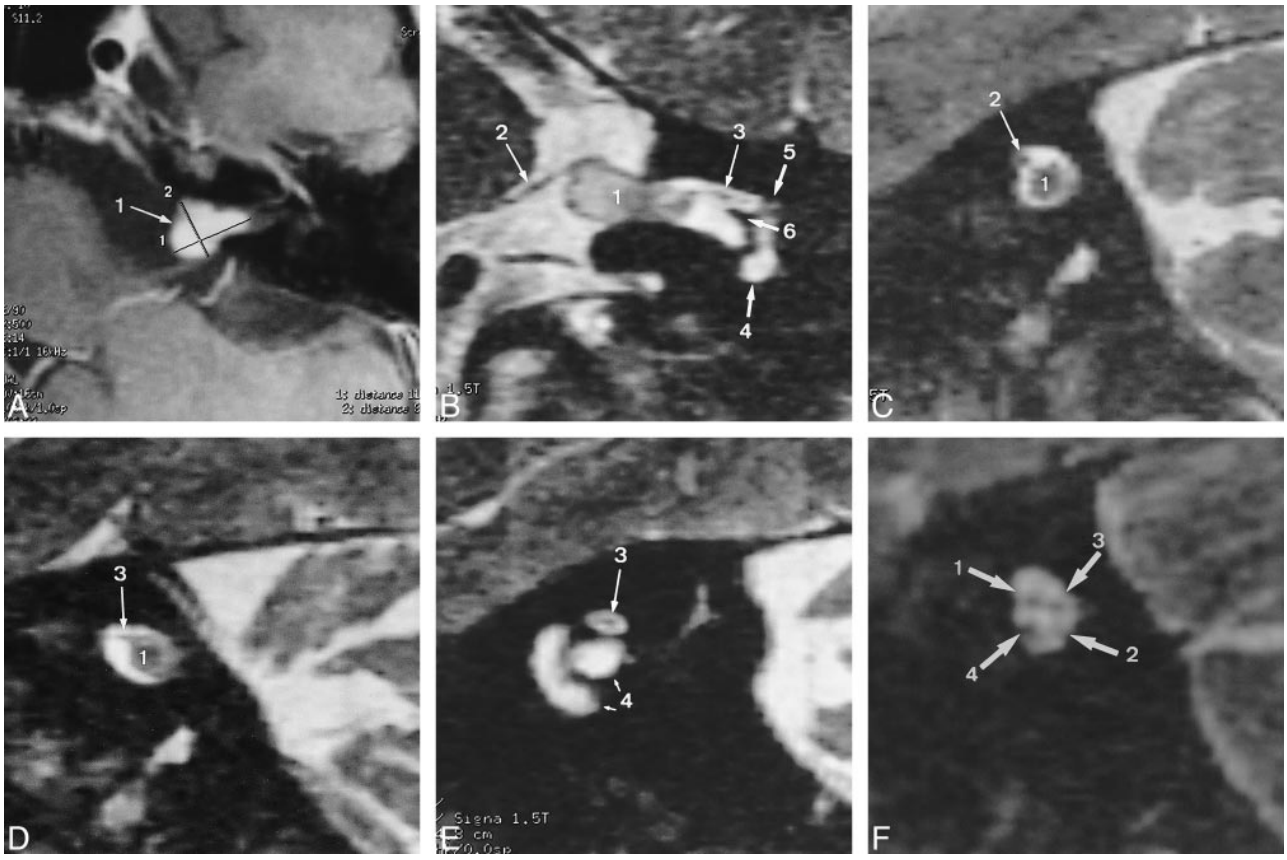

FIG 1. *A,* Postcontrast T1-weighted transverse MR image (600/16/4) shows a vestibular schwannoma (*large 1*), 11 × 8 × 5 mm in size, with both intra- and extrameatal tumor portions (*crosshatches 1* and *2* indicate the measured tumor diameters).

B, Reformatted oblique coronal 3D T2-weighted FSE image (4000/150/1) shows the facial nerve (*2, 3*) in an anterosuperior position within the IAC in relation to the tumor (*1*). The medial (*2*) and lateral (*3*) segments are delineated. The nerve has a normal diameter of 1 mm along the medial segment and the medial part of the intervening segment (*2*), and is focally thinned along the lateral segment and the lateral part of the intervening segment (*3*). The signal intensity of the thinned lateral segment (*3*) is slightly increased relative to the medial segment (*2*) and to the contralateral lateral facial nerve segment (see Fig 1F). The cochlea (*4*), meatal foramen (*5*), and crista falciformis (*6*) are depicted.

C–E, Reformatted oblique sagittal images from medial to lateral.

C, Reformatted oblique sagittal 3D T2-weighted FSE image (4000/150/1) along the medial part of the intervening segment. The facial nerve (*2*) is located anterosuperiorly relative to the tumor (*1*).

D, Reformatted oblique sagittal 3D T2-weighted FSE image (4000/150/1) along the lateral part of the intervening segment. The facial nerve (*3*) is still in an anterosuperior position relative to the tumor (*1*) and is focally thinned with slightly increased signal intensity as compared with the medial segment or with the contralateral facial nerve segment (see Fig 1F).

E, Reformatted oblique sagittal 3D T2-weighted FSE image (4000/150/1) along the lateral nerve segment (*3*) shows a focally thinned lateral nerve segment with slightly increased signal intensity at the entrance of the nerve into the meatal foramen. *4* indicates the cochlea.

F, For comparison, reformatted oblique sagittal 3D T2-weighted FSE image (4000/150/1) through the IAC shows the normal contralateral facial nerve (*1*) as well as the inferior (*2*) and superior (*3*) vestibular nerve and the cochlear nerve (*4*).

on differences in the postprocessing of the various sequences) or on anatomic characteristics (ie, tumor size and location)? The correct position of the facial nerve was verified by placing it either medially (at the nerve root exit zone) or laterally (at the meatal foramen where the nerve enters its bony canal) to the tumor in its typical anatomic location. In comparing T1-weighted postcontrast SE images with T2-weighted images (obtained as a 3D T2-weighted FSE sequence with a section thickness of 0.7 mm and secondary multiplanar reformations with a minimal section thickness of 0.4 mm), we found that the spatial relationship between facial nerve and tumor was depicted only on the 3D T2-weighted FSE images; the facial nerve was not reliably seen on the postcontrast T1-weighted SE images. The reformatted images allowed delineation of the facial nerve parallel and perpendicular to its course on multiple contiguous images, which were thinner than the source image itself. Therefore, delineation of the course of the facial nerve was not analyzed on the coronal source images.

On oblique sagittal (parasagittal) images perpendicular to the long axis of the IAC, it was even possible to observe the nerve every 0.4 mm after its exit from the brain stem to its entrance into the petrous bone. In 86% of the patients the position of the facial nerve in relation to the vestibular schwannoma within the IAC and the CPA cistern could be identified on these very thin and refor-

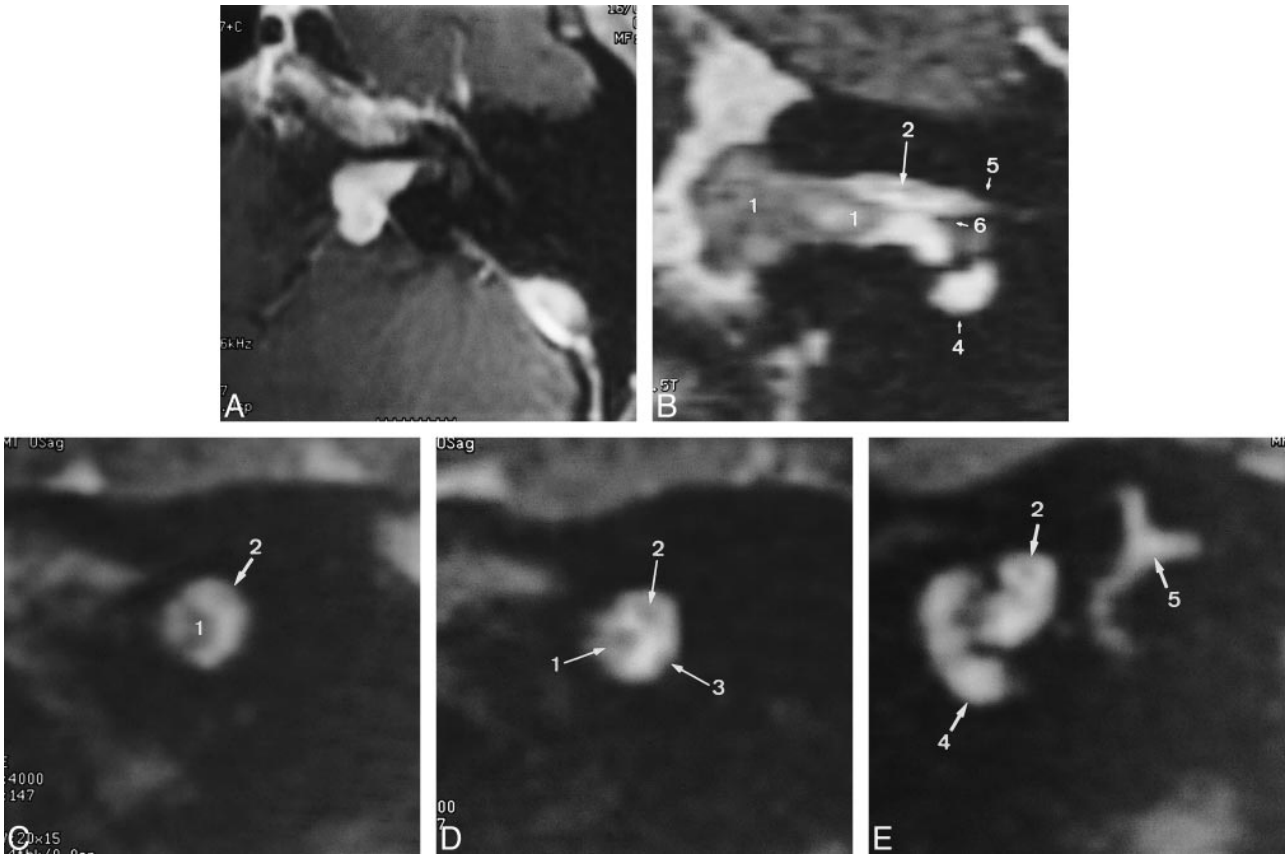

FIG 2. *A,* Postcontrast transverse T1-weighted SE image (600/16/4) shows the intra- and extrameatal location of a vestibular schwannoma (size, 12 × 10 × 7 mm).

B, Reformatted oblique coronal 3D T2-weighted FSE image (4000/150/1) shows the vestibular schwannoma (*1*) and the lateral part of the intervening segment as well as the lateral segment of the facial nerve (*2*). The nerve is slightly hyperintense relative to the contralateral lateral facial nerve segment (not shown). Cochlea (*4*), meatal foramen (*5*), and crista falciformis (*6*) are depicted.

C, Reformatted oblique sagittal 3D T2-weighted FSE image (4000/150/1) along the intervening facial nerve segment (*2*) shows the vestibular schwannoma (*1*) and the facial nerve shifted to a posterosuperior position. The vestibular nerve is not identified.

D, Reformatted oblique sagittal 3D T2-weighted FSE image (4000/150/1) along the intervening facial nerve segment (*2*), lateral to *C,* again shows the vestibular schwannoma (*1*) and the facial nerve (*2*) shifted to a posterosuperior position. The vestibular nerve (*3*) may be assumed to be in a posteroinferior position.

E, Reformatted oblique sagittal 3D T2-weighted FSE image (4000/150/1) along the lateral facial nerve segment (*2*) shows the facial nerve proximal to its entrance into the bony canal at the meatal foramen. Cochlea (*4*) and semicircular canals (*5*) are depicted.

matted 3D T2-weighted FSE images. According to our limited experience (based on analysis of the spatial relationship between tumor and nerve in 22 patients), delineation of the facial nerve and its course was more easily obtained on parasagittal images (8) than on oblique transverse and oblique coronal images. Oblique sagittal images allowed simultaneous demonstration of multiple, or of all four, nerves within the IAC (namely, the facial nerve, the inferior and superior vestibular nerves, and the cochlear nerve). However, in all cases, oblique reformatted images in all three planes were needed for optimal depiction of the nerve and its position along the entirety of its course.

Our results indicate that correct identification of the facial nerve in relation to the tumor depends not only on acquisition and reformation of a 3D T2-weighted FSE series but also on tumor size and location. As a general rule, the smaller the tumor size the more reliable the identification of the nerve within the CPA cistern and the ICA. Three different categories of findings were identified. First, in tumors with a maximal diameter of less than 11 mm, the position of the entire facial nerve adjacent to the vestibular schwannoma was usually correctly determined if the tumor did not fill the entire width of the IAC. Second, if the tumor completely filled and obstructed the IAC and the CPA cistern, as was seen in three of our patients, the facial nerve could not be delineated. And third, if the tumor filled parts of the IAC and the CPA cistern, the nerve was usually identified laterally or medially to the tumor, even if the tumor size exceeded 10 mm. Therefore, single segments of the facial nerve were always identified if the maximal tumor diameter ranged from 10 to 30 mm. Identification of the intervening segment was only possible if the size of the tumor did not exceed 11 mm. Among the three categories of findings, maximal tumor size did overlap to a certain degree.

Vestibular schwannomas may arise within the IAC, at the internal acoustic meatus, or, uncom-

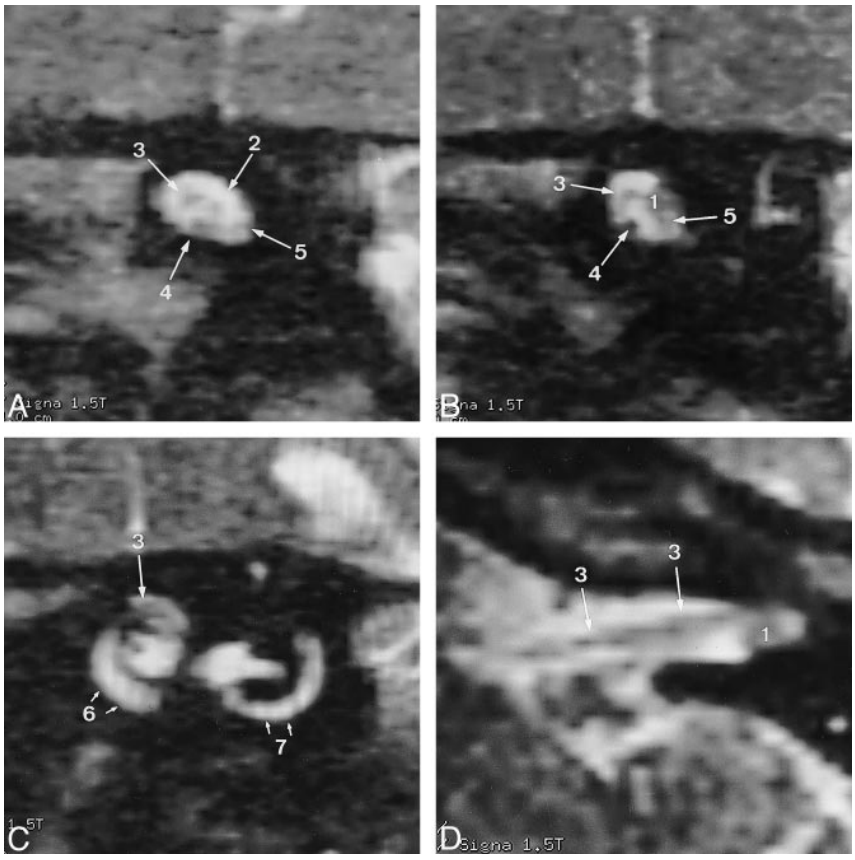

FIG 3. *A,* Reformatted oblique sagittal 3D T2-weighted FSE image (4000/150/1) medial to the tumor shows the superior vestibular nerve (*2*), the facial nerve (*3*), the cochlear nerve (*4*), and the inferior vestibular nerve (*5*). The facial nerve has a normal diameter and does not show increased signal intensity.

B, Reformatted oblique sagittal 3D T2-weighted FSE image (4000/150/1) along the intervening facial nerve segment shows a small vestibular schwannoma (*1*) (mean diameter, 3 mm). The tumor most probably arises from the superior vestibular nerve. The facial nerve along its intervening segment (*3*) is depicted in an anterosuperior position. The cochlear nerve (*4*) and the inferior vestibular nerve (*5*) are depicted.

C, Reformatted oblique sagittal 3D T2-weighted FSE image (4000/150/1) lateral to the tumor shows the lateral segment of the facial nerve (*3*) just proximal to the entrance of the nerve into the bony canal at the meatal foramen. Cochlea (*6*) and semicircular canal (*7*) are depicted.

D, Reformatted oblique coronal 3D T2-weighted FSE image (4000/150/1) shows the facial nerve (*3*) along its medial segment as well as along the intervening segment adjacent to the vestibular schwannoma (*1*). The nerve is in an anterosuperior position.

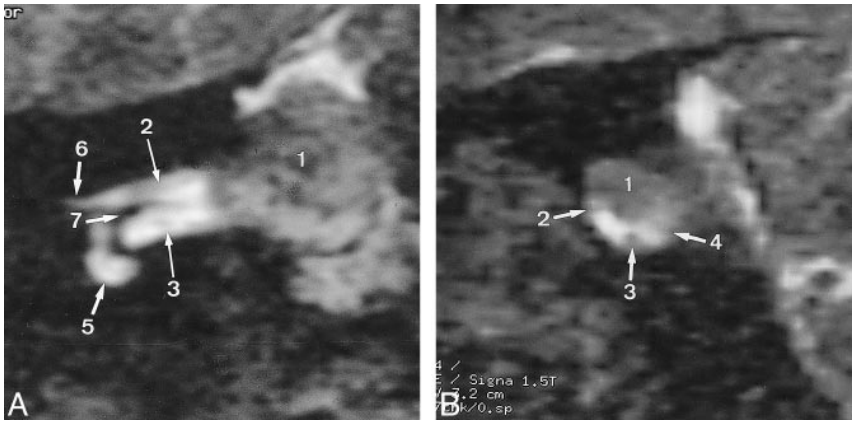

FIG 4. *A,* Reformatted oblique coronal 3D T2-weighted FSE image (4000/150/1) shows the intra- and extrameatal location of a vestibular schwannoma (*1*) (size, 13 × 18 × 11 mm). The lateral segment of the facial nerve (*2*) and the cochlear nerve (*3*) are depicted, as are the cochlea (*5*), meatal foramen (*6*), and crista falciformis (*7*).

B, Reformatted oblique sagittal 3D T2-weighted FSE image (4000/150/1) shows the vestibular schwannoma (*1*) and the facial nerve along its intervening segment (*2*). Because of its position, the tumor (*1*) most probably arises from the superior vestibular nerve; the facial nerve is shifted to an anteroinferior position. The cochlear nerve (*3*) and the inferior vestibular nerve (*4*) are also depicted.

monly, within the CPA cistern. The tumor arises from Schwann cells, which only cover the nerve laterally. Medially, the nerve is covered by neuroglial cells (2, 6, 7). Thus, the facial nerve is more commonly shifted by tumor located within the IAC, as tumors arising from the lateral nerve segment occur more frequently. Identification of the nerve along its free medial segment is much more difficult in these cases, owing to the more variable position of the facial nerve (2, 6, 7). Obviously, even rather small tumors within the IAC, with a maximal diameter of only slightly more than 10 mm, could prevent identification of the lateral and intervening facial nerve segment, as, in our series, they filled and obstructed the entire IAC. In tumors originating within the CPA cistern without extension into the IAC, only larger tumors (with a maximal diameter $>$ 20 mm) did not allow identification of all nerve segments.

Focal facial nerve thinning around the tumor capsule made identification of the nerve even more difficult (1, 2). In 41% of our patients, focal nerve thinning was obvious along the distal intrameatal nerve segment (ie, distal to the tumor itself). Differentiation of the nerve from CSF and tumor was also made difficult by the slightly increased signal intensity of the thinned nerve segment.

Our study shows that demonstration of the spatial relationship between facial nerve and adjacent vestibular schwannoma is possible. The entire nerve course can only be depicted on very thin reformatted 3D T2-weighted FSE images when adjacent to small tumors (maximal size, 11 mm) that do not obstruct the full diameter of the IAC. Identification of the entire nerve or of some nerve segments may be obscured by very large tumors that fill the IAC and/or CPA cistern, especially if additional focal nerve thinning and flattening is present.

Our results are limited by a lack of intraoperative surgical verification. Comparison of radiologic and intraoperative findings is crucial for definitive confirmation of our results; unfortunately, however, such a comparison could not be made because the patients in this series will not undergo surgery, owing to the small size of their tumors and to the minor nature of their clinical deficits. Therefore, we had to rely on previously published anatomic and surgical descriptions of the spatial relationship between vestibular schwannoma and facial nerve (1–7).

Conclusion

For small tumors, the spatial relationship between tumor and nerve can be easily ascertained intraoperatively. Therefore, for these tumors, high-resolution reformatted 3D T2-weighted FSE MR images depicting the spatial relationship between nerve and tumor are not essential for preoperative planning. On the other hand, for large tumors and associated facial nerve thinning, in which intraoperative nerve identification is very difficult, reformatted 3D T2-weighted FSE MR images do not give the required preoperative information about the spatial relationship between nerve and tumor. Thus, the practical value of our results is unclear. Further technical improvements in scanner software will be necessary to accurately show the position of the facial nerve relative to tumors larger than 1 cm, and additional work is required to better define the characteristics that allow a thorough preoperative analysis of the spatial relationship between facial nerve and tumor.

References

1. Fisch U, Mattox D. In: Fisch U, Mattox D, eds. *Microsurgery of the Skull Base.* New York: Thieme Medical;1988:74–131
2. Yasargil MG. **Acoustic neuromas.** In: Yasargil MG, ed. *Microneurosurgery.* New York: Thieme Medical;1996;IVB:100–123
3. Rhoton AL. **Microsurgical anatomy of acoustic neuromas.** *Neurol Res* 1984;6:3–21
4. Rhoton AL. **Microsurgical anatomy of the brainstem surface facing an acoustic neuroma.** *Surg Neurol* 1986;25:326–339
5. Rhoton AL, Tedeschi H. **Microsurgical anatomy of acoustic neuroma.** *Otolaryngol Clin North Am* 1992;25:257–294
6. Rhoton AL. **Microsurgery of the internal acoustic meatus.** *Surg Neurol* 1974;2:311–318
7. Rhoton AL. **The suboccipital approach to removal of acoustic neuromas.** *Head Neck Surg* 1979;1:313–333
8. Naito Y, Miura M, Funabiki K, Naito E, Honjo I. **Application of parasagittal surface coil MRI to otoneurological diagnosis.** *Acta Otolaryngol Suppl (Stockh)* 1997;528:85–90
9. Rauschning W. **Brain tumors and tumorlike masses: classification and differential diagnosis.** In: Osborn AG, ed. *Diagnostic Neuroradiology.* St Louis: Mosby;1994:401–528
10. Brogan M, Chakeres DW. **Gd-DTPA enhanced imaging of cochlear schwannoma.** *AJNR Am J Neuroradiol* 1990;11:407–408
11. Stack JP, Ramsden RT, Antoun NM, Isherwood K, Jenkins JPR. **MRI of acoustic neuromas: the role of gadolinium-DTPA.** *Br J Radiol* 1988;61:800–805
12. Dobson MJ, Hutchinson CE, Adams JE. **Problem in diagnostic imaging: have you got the nerve?** *Clin Anat* 1997;10:345–348